# Monte Carlo simulation study of reflection-electron-energy-loss-spectroscopy spectrum

Z.-J. Ding*
*CCAST (World Laboratory), P.O. Box 8730, Beijing, 100080*
*and Department of Astronomy and Applied Physics, University of Science and Technology of China, Hefei 230026, Anhui, China*

R. Shimizu
*Department of Applied Physics, Osaka University, Suita 565-0871, Osaka, Japan*
(Received 9 September 1998; revised manuscript received 12 December 1999)

The study of inelastic scattering of electrons moving in a surface region is important to a comprehensive understanding of the basic process of electron-surface interaction in a surface electron spectroscopy. A numerical formalism was previously developed to calculate the complex electron self-energy near a metal surface. This inhomogeneous self-energy in the depth about the surface is formulated in terms of a wave-vector-dependent dielectric function which is obtained from the optical data. In this paper, we present a numerical calculation result on the spatially varying differential inelastic scattering cross section and the inelastic mean free path. Combining this inelastic scattering cross section and the Mott cross section for electron elastic scattering has led to a Monte Carlo simulation model for electron interaction with a surface. To verify this simulation model we have carried out simulations of reflection-electron-energy-loss spectroscopy (REELS) spectra for Au and Si, and compared the results with the experimental spectra. The comparison of the spectra shape for Au is quite reasonable. Several surface features for Au having lower-energy losses have been clearly identified, while the higher-energy loss peaks are shown to be mainly of the bulk feature. The simulation result indicates that the energy-loss process of electron in the vacuum region after leaving from a surface makes a dominant contribution to the surface excitation peaks observed in a REELS spectrum.

## I. INTRODUCTION

Surface electron spectroscopies, including Auger electron spectroscopy (AES), x-ray photoelectron spectroscopy (XPS), and the reflection-electron-energy-loss spectroscopy (REELS), have been widely used in the modern surface characterization of materials. In such a spectroscopy surface electronic excitation by scattering electrons is a common effect, which accompanies bulk electronic excitation. The relative contribution to the energy-loss processes of electrons from surface and bulk mode excitations depends strongly on an experimental configuration. The surface effect becomes more important with decreasing primary-electron-beam energy and an increasing angle of incidence. In order to understand the surface energy-loss features presented in AES, XPS, and REELS spectra as well as perform a more accurate quantitative chemical analysis, a detailed knowledge of an electron inelastic scattering cross section at a sample surface and a comprehensive understanding of the electron-surface interaction process are necessary. Such a theoretical study will be essential to extract the signal or background due to the surface excitation from the overall spectrum.

For studying the interaction process of electrons with a solid, a Monte Carlo simulation technique has been the most powerful tool.[1] This technique allows the simulation of multiple scattering processes of electrons in a bulk material quite well,[2,3] due to the abundant knowledge of electron interaction with atoms and solid electrons. However, the understanding of electron-surface interaction is comparatively less and, hence, the simulation study is still quite limited. The present work aims to extend the simulation to include the surface effect of electron inelastic scattering, and this make the simulation more accurate for application to surface analysis.

In this paper, we will first describe the present theory of electron inelastic scattering, that takes into account the surface excitation effect, and a Monte Carlo method that is modified to accommodate the local inelastic mean free path near a surface. Then the numerical calculation results of an inelastic scattering cross section obtained from the imaginary part of the complex self-energy are presented. We consider the cases of electrons penetrating a surface from both the vacuum side and the solid side at an arbitrary incident angle or takeoff angle. Finally, a comparison is made between the experimental angular resolved REELS spectra and a Monte Carlo simulation result for Au and Si.

## II. THEORY

Early theories[4–14] of electron inelastic scattering at a surface concern only free-electron-like samples and/or a simple trajectory geometry, i.e., a movement of the charge normal and parallel to the surface. Several models of electron inelastic scattering, including surface excitation, were recently suggested.[15–22] In some of these an averaging over electron trajectories was carried out,[15–18] leading to a cross section as the function of the path length that an electron traveled.

Considering the fact that, by the orthogonality of the surface and bulk eigenmodes,[23] the bulk-excitation mode transits to the surface-excitation mode while an electron crosses a surface, a comprehensive theory should provide a scattering cross section depending on the depth from the surface.

 

Because the surface plane destroys the isotropic property of the space, the surface excitation probability also depends on the direction in which the electron moves. We further require the theory to be general in form, and applicable to any real metal of a known dielectric constant. A semiclassical expression derived by Chen and co-workers[20,21] does not actually satisfy the boundary condition for the electric displacement. An extension[24–26] of the quantum theory of Flores and Garcia-Moliner[27] for the electron self-energy at a surface provides complete information about the position and angular dependences of the cross section. In the following we shall briefly summarize the theory for the numerical calculation of the inelastic scattering cross section.

Let the specimen be defined in a semi-infinite space of $z<0$. An electron moves with a velocity vector $\mathbf{v}=(\mathbf{v}_\parallel, v_\perp)$, where $\mathbf{v}_\parallel$ is the parallel component and $v_\perp$ the normal component to the surface. In the specular surface reflection model[28,29] the induced potential is determined by the real charge, its image charge, and the fictitious surface charges fixed by the boundary conditions. The image charge and the surface charges are responsible for the surface effect of electron inelastic scattering in the surface region.

General discussions on the surface response function and the electron self-energy have been made previously.[30–32] Assuming a vanishing surface potential and a fast-electron approximation, the random-phase-approximation self-energy of an inhomogeneous system is expressed in terms of the bulk dielectric function of the specimen, for the cases of an electron moving toward the surface from the vacuum side[27] and from the solid side,[25] and for the cases of an electron in the vacuum and in the solid, respectively, as follows:

$$\Sigma(z)=\begin{cases}\Sigma_1(z) & (z>0,\ v_\perp<0)\\ \Sigma_1(z)+\Sigma_2(z) & (z>0,\ v_\perp>0)\\ \Sigma^b+\Sigma^i(z)+\Sigma^s(z)+\Sigma^{i-s}(z) & (z<0,\ v_\perp<0)\\ \Sigma^b+\Sigma^i(z)+\Sigma^s(z) & (z<0,\ v_\perp>0)\end{cases}$$

where $\Sigma^b$, $\Sigma^i(z)$, and $\Sigma^s(z)$ are the position-independent bulk term, the image charge term and the surface charge term [see Eqs. (22)–(24) in Ref. 25], respectively. Therefore, in the case of electron moving toward the surface from the interior of the medium, the image-charge term and the surface charge term are found to represent the net surface effect. In the case of an electron penetrating into the surface from the vacuum side, the surface terms are complicated in form by the interference of the image charge and the surface charges. The extra term representing the interference is

$$\Sigma^{i-s}(z)=\frac{2i}{(2\pi)^3}\int d\mathbf{q}_\parallel\int_0^\infty d\omega \tag{1}$$

$$\times\Bigg\{-2\varepsilon_s(\mathbf{q}_\parallel,\omega)\frac{q_\parallel}{\pi}\int_{-\infty}^{\infty}\frac{e^{iq_\perp z}dq_\perp}{q^2\varepsilon(\mathbf{q},\omega)}$$

$$\times\Bigg[\frac{\pi}{q_\parallel}\left(\frac{e^{-i(\omega-\mathbf{q}_\parallel\cdot\mathbf{v}_\parallel)z/v_\perp}}{\omega-\mathbf{q}_\parallel\cdot\mathbf{v}_\parallel+iq_\parallel v_\perp}-\frac{e^{i(\omega-\mathbf{q}_\parallel\cdot\mathbf{v}_\parallel)z/v_\perp}}{\omega-\mathbf{q}_\parallel\cdot\mathbf{v}_\parallel-iq_\parallel v_\perp}\right)$$

$$+\int_{-\infty}^{\infty}\frac{e^{-i(\omega-\mathbf{q}_\parallel\cdot\mathbf{v}_\parallel)z/v_\perp}dq_\perp}{q^2\varepsilon(\mathbf{q},\omega)(\omega-\mathbf{q}\cdot\mathbf{v}-i\eta)}$$

$$-\int_{-\infty}^{\infty}\frac{e^{i(\omega-\mathbf{q}_\parallel\cdot\mathbf{v}_\parallel)z/v_\perp}dq_\perp}{q^2\varepsilon(\mathbf{q},\omega)(\omega-\mathbf{q}\cdot\mathbf{v}+i\eta)}\Bigg]$$

$$+\int_{-\infty}^{\infty}\frac{e^{-i(\omega-\mathbf{q}_\parallel\cdot\mathbf{v}_\parallel)z/v_\perp}(e^{iq_\perp z}+e^{-iq_\perp z})dq_\perp}{q^2\varepsilon(\mathbf{q},\omega)(\omega-\mathbf{q}\cdot\mathbf{v}-i\eta)}$$

$$-\int_{-\infty}^{\infty}\frac{e^{i(\omega-\mathbf{q}_\parallel\cdot\mathbf{v}_\parallel)z/v_\perp}(e^{iq_\perp z}+e^{-iq_\perp z})dq_\perp}{q^2\varepsilon(\mathbf{q},\omega)(\omega-\mathbf{q}\cdot\mathbf{v}+i\eta)}\Bigg\},$$

where the surface dielectric function $\varepsilon_s(\mathbf{q}_\parallel,\omega)$ is defined from the bulk dielectric function $\varepsilon(\mathbf{q},\omega)$. When an electron moves in the bulk region and is far from the surface, these surface terms tend to cancel each other so that only the bulk scattering term remains. When an electron is in the vacuum region, $\Sigma_1(z)$ [Eq. (28) in Ref. 25] is the classical self-energy for an electron incident onto and escaping from the surface, and the extra term now is $\Sigma_2(z)$ [Eq. (29) in Ref. 25], which also contains the contribution from both the image charge and the surface charges.

We can prove that the continuity equation holds for the total self-energy at the surface,

$$\Sigma(z=0^-,v_\perp)=\Sigma(z=0^+,v_\perp), \tag{2}$$

and, in the case of the parallel movement of an electron to the surface,

$$\Sigma(z,v_\perp=0^-)=\Sigma(z,v_\perp=0^+). \tag{3}$$

It should be noted that each surface self-energy term, $\Sigma_1$, $\Sigma^i$, and $\Sigma^s$, has different values for the same magnitude of vertical velocity but with opposite sign, because the sign of $v_\perp$ affects the analytic property of the terms. Physically, this may be easily understood from the consideration of the asymmetry of the space. Thus $\Sigma_1(v_\perp)=-\Sigma_1(-v_\perp)$ holds. To have a numerically calculable expression of the self-energy, a model complex dielectric function $\varepsilon(\mathbf{q},\omega)$ must be introduced. Because in a surface excitation problem an electron loses energy $\omega$ and changes the parallel momentum $\mathbf{q}_\parallel$, the integration over $q_\perp$ may be carried out analytically. The contour integration is specific to the expression of the dielectric function by the analytic property of the integrand.

We first derived an expression of the self-energy with a Drude-Lindhard model dielectric function for a free-electron-metal.[25] In order to obtain the necessary information concerning electron inelastic scattering in a real metal, an effective method has been devised to use the experimental data on an optical dielectric function $\varepsilon(\omega)$, and to extrapolate it from the optical limit to other momentum transfer.[33] In the present work we used the method proposed by Ritchie and Howie[34] to obtain an approximate energy-loss function for arbitrary $q$ values from an optical energy-loss function, $\mathrm{Im}\{-1/\epsilon(\omega)\}$. In brief, a fitting procedure with a SIMPLEX optimizing routine[35] to the experimental data is made to obtain the parameters involved in a sum of Drude-Lindhard model energy-loss functions at $q=0$. Further extending to finite $q$ values by assuming a plasmon dispersion results in the required $\varepsilon(\mathbf{q},\omega)$.

According to this scheme the surface dielectric function $\varepsilon_s(\mathbf{q}_\parallel,\omega)$ satisfies the surface $f$-sum rule and the surface perfect-screening sum rule along with the corresponding bulk sum rules satisfied by the bulk dielectric function.

The inelastic scattering cross-section differential in $\mathbf{q}_\parallel$ and $\omega$ may be obtained from the imaginary part of the differential self-energy as

$$\sigma(\mathbf{q}_\parallel,\omega|z,\mathbf{v}) = -2v^{-1}\,\mathrm{Im}\{\Sigma(\mathbf{q}_\parallel,\omega|z,\mathbf{v})\}, \tag{4}$$

where the triple differential self-energy $\Sigma(\mathbf{q}_\parallel,\omega|z,\mathbf{v})$ is the integrand appeared in the self-energy integral expression. The left half of the parentheses in the above notation indicates the variables with respect to which the differentiation is taken, and the right half the parameters that the self-energy depends on. We may perform integration over the angle between $\mathbf{q}_\parallel$ and $\mathbf{v}_\parallel$ to derive the double-differential cross section $\sigma(q_\parallel,\omega|z,\mathbf{v})$. The differential cross section in energy loss and the inverse of the inelastic scattering mean free path are obtained numerically from the integration

$$\lambda_{\mathrm{in}}^{-1}(z,\mathbf{v}) \equiv \sigma_{\mathrm{in}}(z,\mathbf{v}) = \int d\omega\,\sigma(\omega|z,\mathbf{v}) = \int dq_\parallel d\omega\,\sigma(q_\parallel,\omega|z,\mathbf{v}). \tag{5}$$

The scattering mean free path is thus local in the surface region. Along with the definition for the bulk one,[36] the local inelastic mean free path may still be considered as the average of the distance that electrons at a certain position travel in a specified direction between inelastic collisions.

## III. MONTE CARLO METHOD

The first step in a Monte Carlo simulation of electron scattering processes is the sampling procedure for the electron flight length $s$ between the successive individual scattering events; a description of a scattering event follows. Note that the inelastic scattering cross section depends on the position of electrons inside both the vacuum and the metal, and an improvement to the sampling technique for the bulk case is necessary that takes into account the local mean free path. Assume that the probability distribution of the flight length obeys an exponential law; the distribution function of $s$ has a general form

$$f(s) = \sigma(s)\exp\left\{-\int_0^s \sigma(s')ds'\right\}. \tag{6}$$

A conventional Monte Carlo sampling technique for $f(s)$ requires solving an accumulation function with a uniform random number $R$. This reduces to $\int_0^s \sigma(s')ds' = -\ln R$, provided that $\sigma(s)$ is positive for all $s>0$; $\int_0^\infty \sigma(s)ds = \infty$, so that $f(s)$ is normalized. However, the equation is difficult to solve efficiently in practice. We then used a fast sampling technique:[37] Now we rewrite Eq. (6) as a distribution function of the electron position. Let $z_0$ be the present position of the electron, and consider the future position $z$ of the electron after traveling a flight length $s$, which is inclined from the surface normal direction with an angle $\alpha$. Therefore, $z - z_0 = s\cos\alpha$. Because $f(s)ds = f(z)dz$, we have the probability distribution of $z$:

$$f(z|z_0,\alpha) = \frac{\sigma(z,\alpha)}{\cos\alpha}\exp\left\{-\int_{z_0}^{z}\frac{\sigma(z',\alpha)}{\cos\alpha}dz'\right\}. \tag{7}$$

The sampling procedure for $z$ is (1) $z=z_0$, (2) $z = z - \cos\alpha \ln R_1/\sigma_m(\alpha)$, and (3) $R_2 \leqslant \sigma(z,\alpha)/\sigma_m(\alpha)$?, where $R_1$ and $R_2$ are two independent random numbers. If step (3) is satisfied, then we accept the value of $z$. Otherwise, we generate another two random numbers and proceed to step (2) until step (3) is satisfied. In the above equation $\sigma_m = \max\{\sigma(z,\alpha)\}$; $\sigma(z,\alpha)$ is the total cross-section, being the sum of the elastic scattering cross section and the inelastic scattering cross section; and $\sigma(z,\alpha) = \sigma_e(v)\Theta(-z) + \sigma_{\mathrm{in}}(z,\mathbf{v})$, where $\Theta(z)$ is a step function.

In the case of an electron leaving the surface toward the vacuum, the integration of the scattering cross section from the electron position to an infinite distance has a finite value, and $f(s)$ is not normalized. The above procedure may result in a nonconvergent recurrence. Physically, this represents the situation of electron emission into the vacuum without any scattering. Therefore, the procedure is still effective except that the recurrence should be terminated when an electron moves far away from the surface.

When $z$ is determined, as well as the path length $s$ and the coordinates of the next scattering position of an electron, we use another random number to choose the type of scattering event according to the ratio of the elastic cross section to the total cross section. The relativistic elastic scattering cross section, the Mott cross section, is calculated by a partial-wave-expansion method.[38] Obviously, an elastic scattering event can only occur underneath the surface, i.e., $z<0$. For such an event, a random number produces a scattering angle from the corresponding differential elastic cross section. The azimuth angle has been assumed to be isotropically distributed. This decides the new direction of the electron movement after the collision with an atom.

For an inelastic event, a random number produces an energy loss from the differential cross section. Rigorously, the new moving direction of the electron should be decided according to the momentum transfer $\mathbf{q} = (\mathbf{q}_\parallel, q_\perp)$ to the surface. This requires a tabulation of the quadruple differential cross section in $\mathbf{q}$ and $\omega$ with a large amount of memory space. Because the angular deflection in an inelastic scattering event is much smaller than that in an elastic scattering event, we then simply estimated this scattering angle according to a binary collision model, $\sin\theta = \sqrt{\omega/E}$. The azimuth angle is derived similarly to the procedure in an elastic scattering event. The successive scattering events form an electron trajectory, which is terminated either when its energy is below the cutoff energy or is backscattered into the vacuum region and far away from the surface. Note that the present simulation model enables an electron inelastic event to occur in the vacuum region and near to the surface. This is the main difference from a conventional bulk model, which assumes that the scattering events occur only inside the solid.

## IV. RESULTS AND DISCUSSION

Numerical calculations of the differential energy-loss cross section and inelastic mean free path have been performed for Au and Si. The dependence on the kinetic energy, the distance from the surface, and the incident angle or take-off angle will be presented below. For Au the surface feature and the bulk feature in an experimental REELS spectrum are hardly to be separated without a detailed theoretical study.

The analysis of the cross section calculated is essential to understanding the Monte Carlo simulation result for the REELS spectra.

An optical energy-loss function usually extends over a wide range of photon energy $\omega$ from $10^0$ to $10^3$ eV. The lower-energy region ($<10^2$ eV) exhibits a complex structure due to interband transitions. Inner-shell ionization edges can be observed at high energies. For a calculation of the inelastic scattering mean free path of keV electrons, the whole photon energy range should be concerned. The total number of Drude-Lindhard terms is large enough so that the fitted energy-loss function represents the optical data quite well up to deep inner-shell edges. The angular integration and the integration over $q_\parallel$ in Eq. (6) are numerically calculated with a Romberg routine. The upper limit of $q_\parallel$ is taken as 1–5 $\text{Å}^{-1}$, at which the double-differential cross section $\sigma(q_\parallel,\omega)$ is quite close to zero.

The differential cross section for Si indicates that, for $z<0$ and $v_\perp>0$, $\sigma^i(\omega)$ contributes positively to the cross section at the bulk plasmon energy, while $\sigma^s(\omega)$ contributes positively at the surface plasmon energy and negatively at the bulk plasmon energy. The term $\sigma^{i-s}(\omega)$ also tends to reduce the bulk component. The net surface effect is thus to build a surface plasmon mode and diminish a bulk plasmon mode beneath the surface. At enough large $|z|$, both $\sigma^i(\omega)$ and $\sigma^{i-s}(\omega)$ oscillate with $\omega$ in such a manner that they cancel each other. Though the situation is quite different from the case of $v_\perp>0$, the effect is the same: only the $z$-independent bulk remains. For $z>0$, $\sigma_1(\omega)$ and $\sigma_2(\omega)$ have a contrary tendency toward surface plasmon excitation.

However, for the noble metal Au, both the bulk and surface modes have rather broadened distributions in the energy loss $\omega$. It is then hard to identify the unique characteristic energy for the surface mode. Figure 1 shows that the main difference between the two modes is that the distribution of the surface mode has a stronger intensity in the lower-$\omega$ region compared with the bulk mode. For $z<0$ and $v_\perp>0$, the surface charge term tends to cancel the image charge term and the bulk term. However, there is an exception for the sharp peak at 2.6 eV that is clearly presented as a surface effect. Though the peak is also observable in the bulk optical energy-loss function, it is only shown as a shoulder in $\sigma^b(\omega)$. Hence the peak at 2.6 eV should be largely associated with the surface mode.

Because $\sigma(\omega|z>0,\ v_\perp<0)=-\sigma_1(\omega|z>0,\ v_\perp>0)$, Fig. 1(a) then indicates that, for $z>0$, the differential scattering cross section is larger for $v_\perp>0$, the case of an electron leaving the surface, than that for $v_\perp<0$, the case of an electron approaching the surface. This behavior of the cross section in relation to the direction in which the electron moves can also be found in the case of $z<0$. The tendency accounts for the angular dependence of the inelastic mean free path. When an electron travels deep inside the metal with $v_\perp>0$, the surface terms all vanish, and only the bulk term remains.

Figure 2 demonstrates the differential cross section for an electron moving in Au and in a direction leaving the surface. There are now three surface terms. By comparing Figs. 2(a) and Fig. 1(b) we can see that the lower-$\omega$ surface mode excitation is more intensive for $\alpha=\pi$ than for the opposite direction, $\alpha=0$. Figure 2(b) shows that, when an electron travels deep inside the metal with $v_\perp<0$, only $\sigma^s$ vanishes

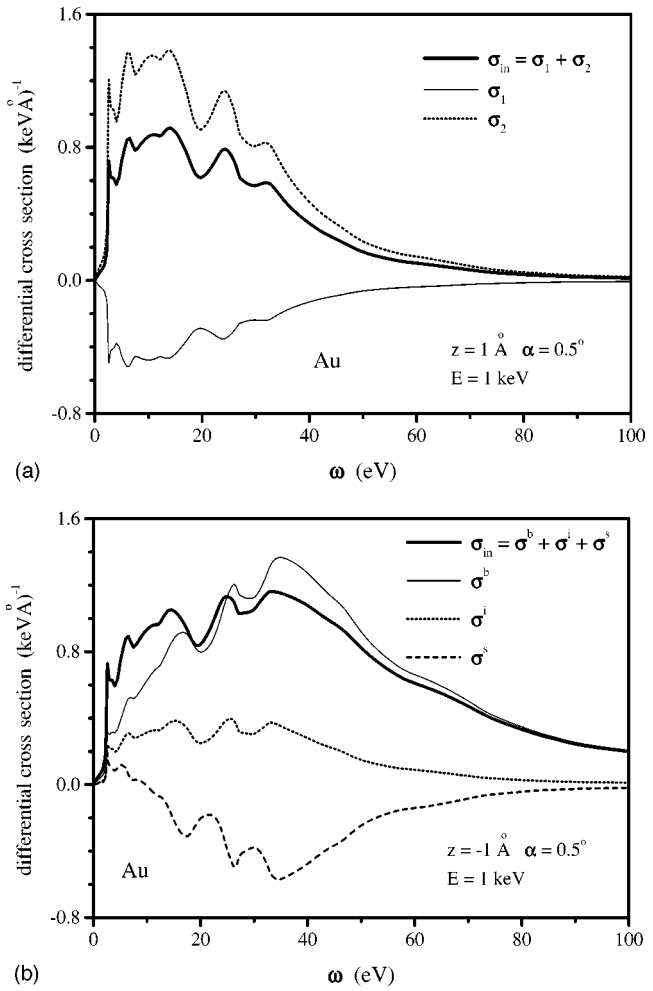


FIG. 1. Differential cross section as a function of $\omega$ for an electron moving to escape an Au sample surface into the vacuum at different positions or directions. $\alpha$ is the angle between the velocity vector and the surface normal direction.

among three surface terms. $\sigma^i(\omega)$ and $\sigma^{i-s}(\omega)$ oscillate with $\omega$ as the oscillation frequency increases with the electron depth. For the parallel movement to the surface, the surface terms can be very small at a large $|z|$. By comparing the differential cross sections for different directions of electron motion, we found that the surface mode excitation ''prefers'' the parallel movement of an electron to the surface. This is due to the resonant interaction of electrons with the plasmon waves, caused by matching the electron velocity and the phase velocity $v_\parallel=\omega/q_\parallel$, when an electron can spend a longer time in its parallel movement.

Figure 3 is a diagram of the $z$ dependence of the differential cross section including the bulk term and all surface terms. For a noble metal having a broad distribution of energy-loss functions, it clearly shows, how a bulk mode excitation spectrum gradually changes into a surface mode spectrum with an electron penetrating the surface. At the geometrical surface, $z=0$, some lower-$\omega$ peaks achieve the maximum height. These peaks, hence, undoubtedly possess a certain surface feature. The lower-$\omega$ peaks extend to the vacuum side over a distance of several nm, but the intensity is still finite even deep inside the solid. For this, they cannot be regarded fully as surface features. Furthermore, the peak position shifts gradually with $z$. Therefore, a peak appearing

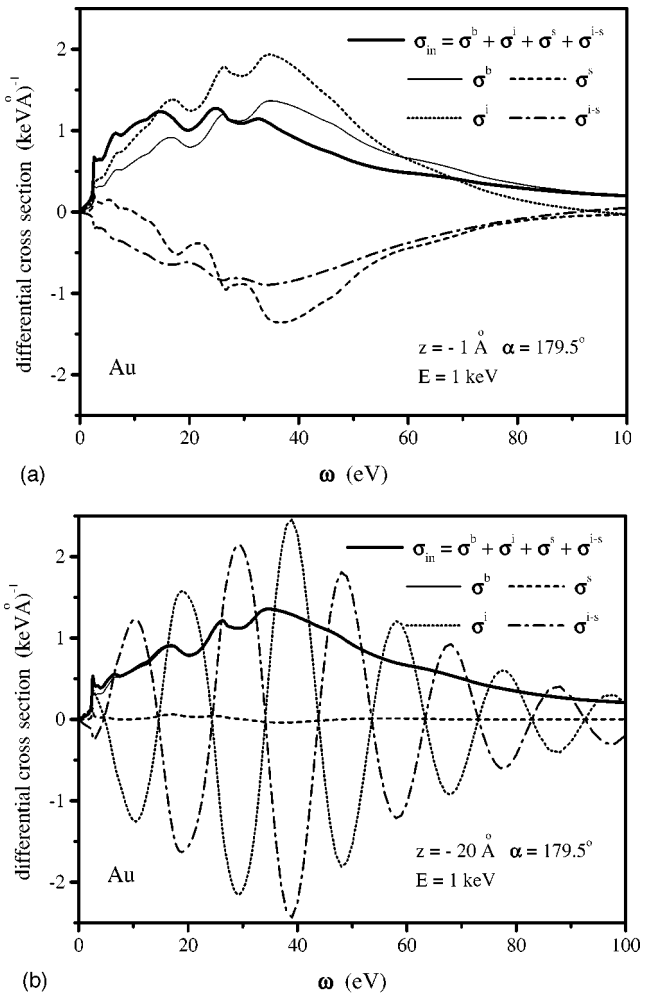


FIG. 2. Differential cross section as a function of $\omega$ for an electron moving to penetrate an Au sample surface into the solid at a different position or direction. $\alpha$ is the angle between the velocity vector and the surface normal direction.

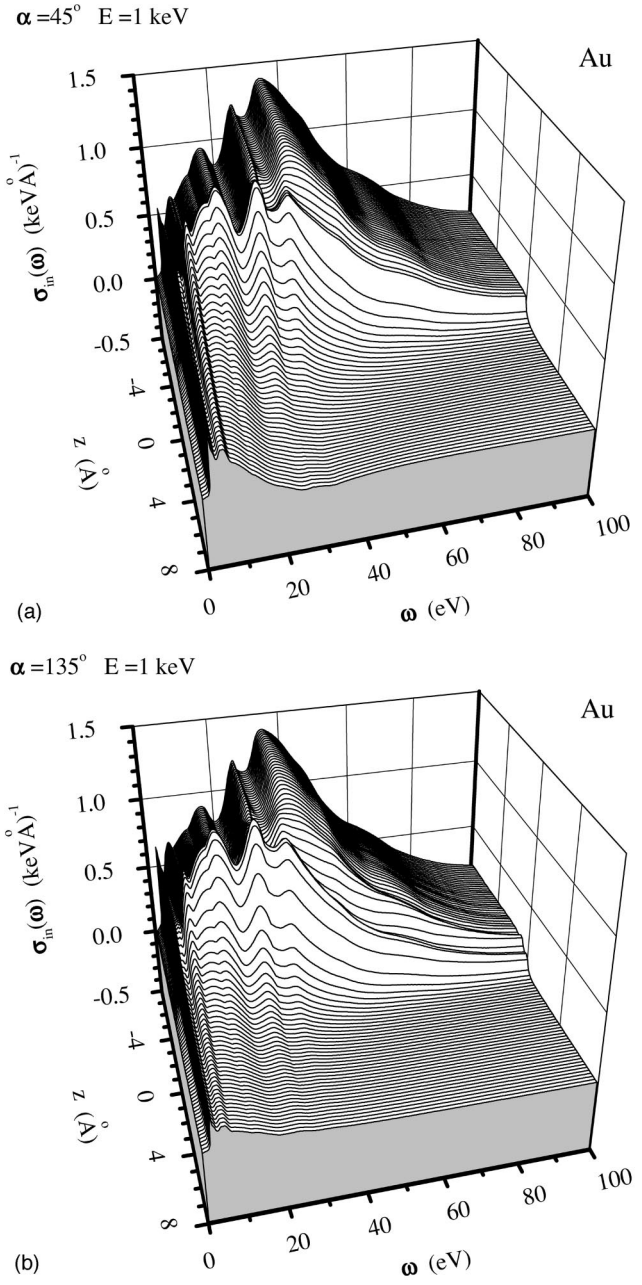


FIG. 3. Perspective view of the differential cross section as a function of $\omega$ and $z$ for an electron penetrating an Au surface (a) from the solid side, and (b) from the vacuum side.

in an experimental REELS spectrum generally comprises both surface and bulk features. Because the energy-loss probability varies continuously with electron movement, the overall energy-loss spectrum of electrons entering into a detector averages the depth dependence of the cross section.

Figure 4 shows the total inelastic cross section, or the inverse of the inelastic mean free path, as the function of $z$ for several typical directions of the electron movement. In the vacuum region, the cross section falls off with an increase of $z$. The tendency agrees with the calculation of Chen and Kwei;[20] however, the quantitative values are quite different: our cross sections are larger in the solid but smaller in the vacuum, and the decrease of the intensity with the increase of $z$ is faster. The angular dependence shows that the cross section at a certain distance $z$ is larger for an electron leaving the surface than one approaching the surface [Fig. 4(a)] For Si, a slight oscillation around the mean value, the bulk cross section, is found [Fig. 4(b)]. This may be associated with the wake behavior of an electron passing through the surface.[39]

For a surface-excitation problem approached by a Monte Carlo simulation method, nearly all studies[40–45] up to now assumed that the excitation takes place only in the solid side as for bulk excitation. However, it has been well recognized[12,13,46–56] that surface excitation can be generated by an electron traveling in the vacuum region. Therefore, it is necessary to clarify the significance of surface excitation in the vacuum part to surface electron spectroscopy. For this purpose the simulation of REELS spectra and a comparison with experimental measurement should be adequate. In a comparison of XPS spectra the backgrounds due to different signal peaks overlap and, in particular, some low-loss surface excitation features may be buried by the following signal peak so that they cannot be resolved. Then the angular-resolved REELS spectra taken under a monoenergetic primary electron beam should be the most appropriate means to exam the theory by checking the energy-loss feature, the

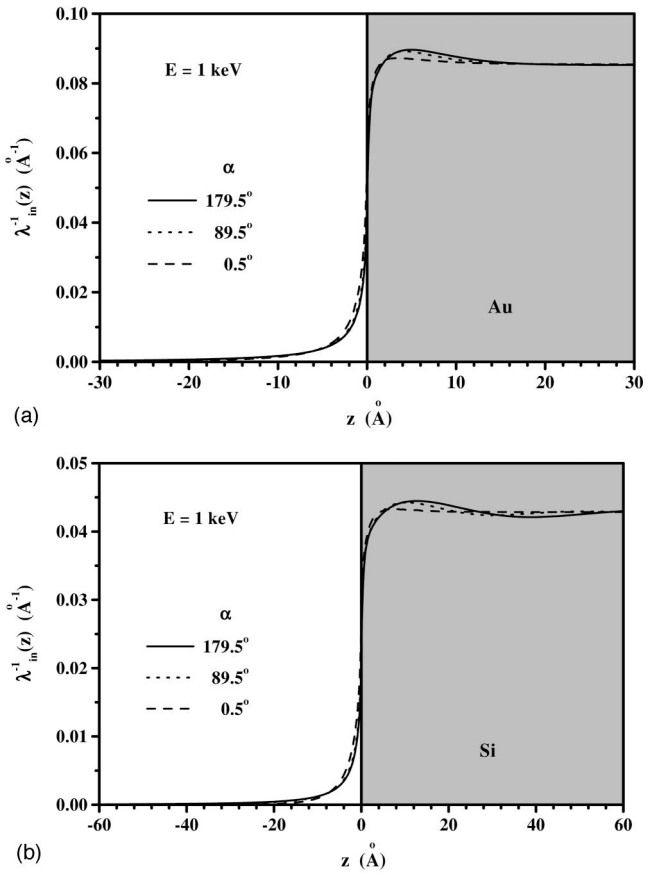


FIG. 4. Total inelastic cross section as a function of $z$ for (a) Au and (b) Si.

takeoff angle dependence, and the incident angle dependence of the cross section.

Monte Carlo simulations were done for REELS spectra of Au and Si. Electron trajectories of as much as $2\times10^9$ were traced in the simulation. The initial position of the incident electrons was set to $z=60$ Å, as at such a distance from the surface the inelastic scattering probability is close enough to zero.

Figure 5 shows the simulated hemispherical REELS spectra for Au. The solid line is the present surface model, i.e., using the present inelastic scattering cross section in the whole space. The dotted line is the result based on our previous bulk model using only the bulk cross-section term, and simulating all the scattering events inside the metal.[2] Dashed and chain lines represent a compromise between the surface model and the bulk model: In the surface-bulk model 2 (dashed line), inelastic scattering events are allowed to occur only inside the metal, using our present inelastic cross section. However, in surface-bulk model 1 (chain line) we further require that the inelastic scattering also occur in the vacuum region, accompanied by the electrons that leave from the surface.

The loss spectrum obtained by the surface model resolves the following surface features: two peaks at 2.8 and 5.7 eV and a hump at 11 eV. Because these features are not obvious in the bulk model, they are largely attributed to the surface excitations. In particular, as mentioned above and demonstrated by Fig. 3, 2.8- and 5.7-eV peaks are obviously due mainly to the surface plasmon,[57] which can be excited by

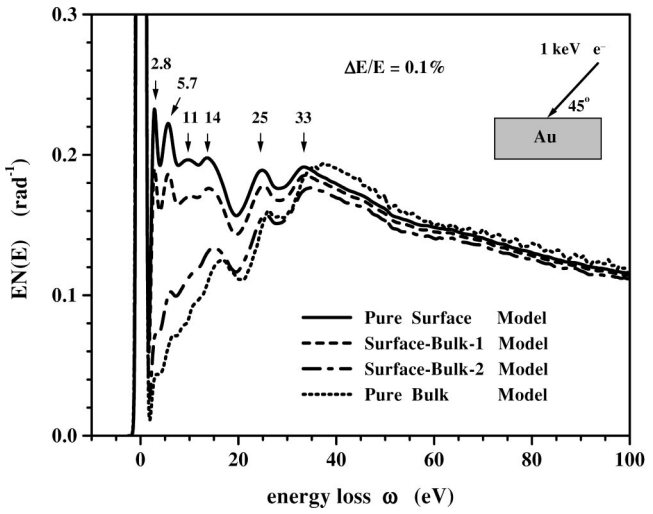


FIG. 5. Monte Carlo simulated REELS spectra for Au and for a 1-keV primary beam. Detection solid angles are hemispherical. The spectra were convoluted with a Gaussian function in a relative energy resolution of 0.1%.

electrons in the vacuum region as well as inside the metal. The component from an interband transition of the bulk Au electrons[58] is quite small. For other peaks at 14, 25, and 33 eV, they include both surface and bulk components; the higher the $\omega$ values the lower the surface mode component. Only the bulk component remains above 35 eV.

We also find that, though surface-bulk model 2 shows a slight contribution of the surface excitation by electrons under a metal surface, the line shape of the spectrum is still quite close to the bulk model. This fact indicates that the surface excitation in the surface model occurs mainly in the course of the movement of electrons in the vacuum region. In particular, the portion of electron trajectories after reflecting into the vacuum is the most important to the surface excitation, as illustrated by the surface-bulk model 1. The present simulation then clarifies the significance of surface excitation in the vacuum region to surface electron spectroscopies.

At a worse energy resolution, the 2.8-eV loss peak may be unresolved. The overall shape of the spectra obtained at such a lower resolution is quite similar to the experimental spectrum measured by Powell[59] for evaporated Au onto a frozen Au substrate.

Figure 6(a) compares the simulated REELS spectra with an experimental measurement for Au.[60] The components of the multiple inelastic scattering in the spectrum are also displayed. The experimental peaks and humps are at positions of 2.8, 6.2, 10.2, 15.9, and 24.6 eV, corresponding to theoretical peaks at 2.6, 5.7, 11, 14, and 25 eV, respectively. The line shapes of the spectrum for the surface feature agree with each other reasonably well. Another comparison with two experimental measurements for Au,[42,61] obtained by varing the takeoff angle, has verified that the theoretical intensity distribution of energy losses larger than 30 eV agrees quite well with experimental spectrum for all takeoff angles. However, the difference in the vacuum condition and the method for preparing a clean surface between the experiment of Ref. 60 and the experiments of Refs. 42 and 61 has led to a quite large difference in the intensity of the surface excitation

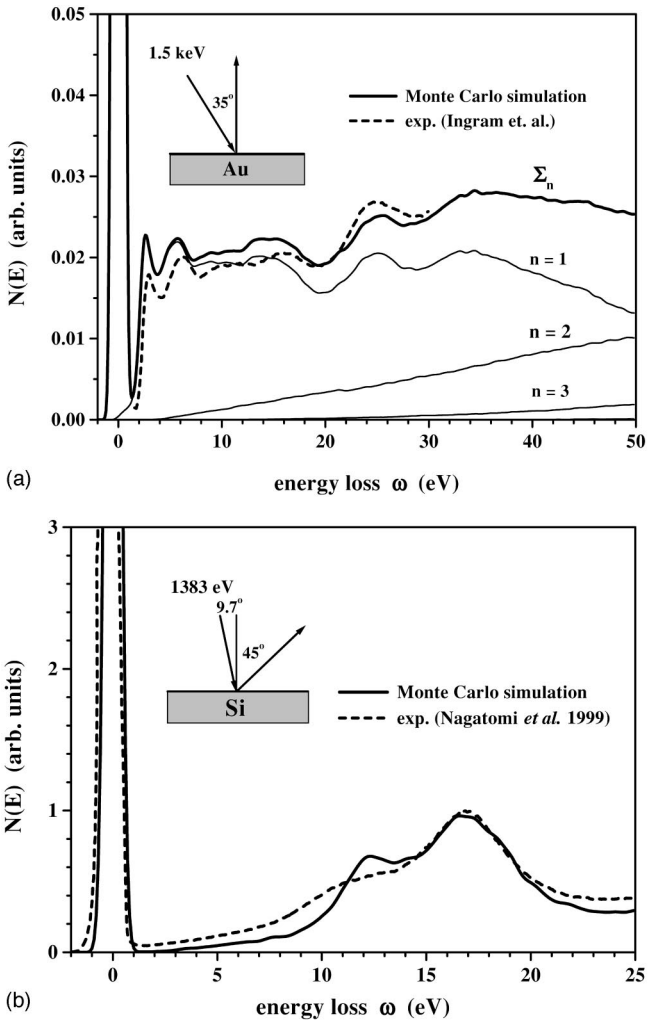


FIG. 6. Comparison between the Monte Carlo simulated angular-resolved REELS spectra (solid line) and an experimental measurement (dashed line). (a) Au. The number $n$ denotes the number of the inelastic scattering event, $\Sigma_n$ is the sum. (b) Si.

peaks. Figure 6(b) shows a similar comparison with the experiment[62] for Si. The measured spectrum[62] for the sputter-cleaned Si(100) surface in a higher vacuum presented a slightly stronger surface plasmon peak intensity than that for the heating-cleaned Si(111) surface in a lower vacuum.[63]

The simulated loss intensity for the surface excitations is still somewhat stronger than the experimental measurement. Despite its sensitivity to the vacuum level that affects the cleanness of the surface, several other factors may account for the difference. First, the surface roughness can damp and broaden the surface peak for an ideal flat surface. In addition, the nonuniform density distribution of solid electrons at the surface[64] can reduce the relative intensity of the surface plasmon peak to the volume plasmon peak for the step model of the surface electron gas.[65] Furthermore, this electronic selvage at a metal surface is known to yield a realistic negative dispersion[66] for small $q_{\|}$, which shifts and broadens the surface loss peak to the lower energies. This shifting of the peak position of the surface plasmon for Si to the lower-energy side is obvious in Fig. 6(b).

## V. CONCLUSION

In conclusion, we have described a theory of electron inelastic scattering near a surface region. The theory provides complete information about the dependence of the total and differential cross sections on the kinetic energy, the distance from the surface, and the moving direction of electrons, accommodating the practical situation in surface electron spectroscopies. Numerical calculation results for the spatially varying differential inelastic scattering cross section and the inelastic mean free path have been given. A Monte Carlo simulation model using a position-dependent scattering cross section was presented. In order to verify the present theory of electron inelastic scattering and the Monte Carlo model, we performed simulations of the angular-resolved REELS spectra, and compared them with several experimental measurements. It was shown that, for Au, features having lower-energy losses are mainly due to the surface mode excitation. The comparison with experiments is reasonable, and a possible reason for the difference was discussed. From the simulation we found that the contribution to the surface excitation peaks in a REELS spectrum by electrons leaving the surface and traveling in the vacuum region is the most prominent feature. This indicates that the surface excitation problem should be important for quantitative AES and XPS analyses.

## ACKNOWLEDGMENTS

The author is grateful to Dr. C. J. Powell for helpful discussion on the REELS spectrum. This work was supported in part by the National Natural Science Foundation of China (Grant Nos. 29675021 and 19674054), the Foundation for High Performance Computing (Grant Nos. 96203 and 970017). Part of the data presented here was calculated with a parallel computer. Dawn-1000, at the High Performance Computing Center at Hefei.

*Electronic address: zjding@ustc.edu.cn

[1] R. Shimizu and Z.-J. Ding, Rep. Prog. Phys. **55**, 487 (1992).
[2] Z.-J. Ding and R. Shimizu, Surf. Sci. **336**, 397 (1995).
[3] Z.-J. Ding and R. Shimizu, Scanning **18**, 92 (1996).
[4] D. M. Newns, Phys. Rev. B **8**, 3304 (1970).
[5] B. Gumhalter and D. M. Newns, Surf. Sci. **50**, 465 (1975).
[6] D. Chan and P. Richmond, J. Phys. C **9**, 163 (1976).
[7] R. Nunez, P. M. Echenique, and R. H. Ritchie, J. Phys. C **13**, 4229 (1980).
[8] P. M. Echenique, R. H. Ritchie, N. Barberan, and J. Inkson, Phys. Rev. B **23**, 6486 (1981).
[9] C. C. Sung and R. H. Ritchie, J. Phys. C **14**, 2409 (1981).
[10] P. M. Echenique, Philos. Mag. B **52**, L9 (1985).
[11] A. Gras-Marti, P. M. Echenique, and R. H. Ritchie, Surf. Sci. **173**, 310 (1986).
[12] P. M. Echenique, J. Bausells, and A. Rivacoba, Phys. Rev. B **35**, 1521 (1987).
[13] N. Zabala and P. M. Echenique, Ultramicroscopy **32**, 327 (1990).
[14] J. L. Gervasoni and N. R. Arista, Surf. Sci. **260**, 329 (1992).
[15] F. Yubero and S. Tougaard, Phys. Rev. B **46**, 2486 (1992).
[16] C. J. Tung, Y. F. Chen, C. M. Kwei, and T. L. Chou, Phys. Rev. B **49**, 16 684 (1994).

[17] Y. F. Chen, J. Vac. Sci. Technol. A **13**, 2665 (1995).
[18] F. Yubero, J. M. Sanz, B. Ramskov, and S. Tougaard, Phys. Rev. B **53**, 9719 (1996).
[19] J. I. Juaristi, F. J. Garcia de Abajo, and P. M. Echnique, Phys. Rev. B **53**, 13 839 (1996).
[20] Y. F. Chen and Y. T. Chen, Phys. Rev. B **53**, 4980 (1996).
[21] Y. F. Chen and C. M. Kwei, Surf. Sci. **364**, 131 (1996).
[22] A. C. Simonsen, F. Yubero, and S. S. Tougaard, Phys. Rev. B **56**, 1612 (1997).
[23] R. H. Ritchie, Phys. Rev. **106**, 874 (1957).
[24] Z.-J. Ding, Phys. Rev. B **55**, 9999 (1997).
[25] Z.-J. Ding, J. Phys.: Condens. Matter **10**, 1733 (1998).
[26] Z.-J. Ding, J. Phys.: Condens. Matter **10**, 1753 (1998).
[27] F. Flores and F. Garcia-Moliner, J. Phys. C **12**, 907 (1979). For the cases $z<0$ and $v_{\perp}<0$, from Eq. (6.11) we derived the final form of the present differential cross section, which is somewhat different from that expressed in Eq. (6.13). The present expression satisfies the continuous conditions mentioned in the text.
[28] R. H. Ritchie and A. L. Marusak, Surf. Sci. **4**, 234 (1966).
[29] F. Garcia-Moliner and F. Flores, *Introduction to the Theory of Solid Surfaces* (Cambridge University, Cambridge, 1979).
[30] B. Gumhalter, Prog. Surf. Sci. **15**, 1 (1984).
[31] R. H. Ritchie, A. Howie, P. M. Echenique, G. J. Basbas, T. L. Ferrell, and J. C. Ashley, Scanning Microsc. Suppl. **4**, 45 (1990).
[32] S. Shindo, Solid State Phenom. **28/29**, 103 (1992).
[33] D. R. Penn, Phys. Rev. B **35**, 482 (1987).
[34] R. H. Ritchie and A. Howie, Philos. Mag. **36**, 463 (1977).
[35] J. A. Nelder and R. Mead, Comput. J. (UK) **8**, 308 (1965).
[36] Standard E 673, *Annual Book of ASTM Standards* (American Society for Testing and Materials, Pennsylvania, 1997), Vol. 3.06.
[37] W. A. Coleman, Nucl. Sci. Eng. **32**, 76 (1968).
[38] Y. Yamazaki, Ph.D. thesis, Osaka University, 1977.
[39] *Handbook of Optical Constants of Solids*, edited by E. D. Palik (Academic, Orlando, 1985).
[40] P. Dubot, D. Jousset, V. Pinet, F. Pellerin, and J. P. Langeron, Surf. Interface Anal. **12**, 99 (1988).
[41] H. Yoshikawa, R. Shimizu, and Z.-J. Ding, Surf. Sci. **261**, 403 (1992).
[42] H. Yoshikawa, T. Tsukamoto, R. Shimizu, and V. Crist, Surf. Interface Anal. **18**, 757 (1992).
[43] K. Tokesi, D. Varga, L. Kover, and T. Mukoyama, J. Electron Spectrosc. Relat. Phenom. **76**, 427 (1995).
[44] T. Nagatomi, Z.-J. Ding, and R. Shimizu, Surf. Sci. **359**, 163 (1996).
[45] J. P. Wang, C. J. Tung, Y. F. Chen, and C. M. Kwei, Nucl. Instrum. Methods Phys. Res. B **108**, 331 (1996).
[46] A. Howie and R. H. Milne, J. Microsc. **136**, 279 (1984).
[47] T. L. Ferrell and P. M. Echenique, Phys. Rev. Lett. **14**, 1526 (1985).
[48] P. E. Batson, Surf. Sci. **156**, 720 (1985).
[49] M. Acheche, C. Colliex, H. Kohl, A. Nourtier, and P. Trebbia, Ultramicroscopy **20**, 99 (1986).
[50] P. M. Echenique, A. Howie, and D. J. Wheatley, Philos. Mag. B **56**, 335 (1987).
[51] R. H. Ritchie, Philos. Mag. A **58**, 753 (1988).
[52] N. Zabala, A. Rivacoba, and P. M. Echenique, Surf. Sci. **209**, 465 (1989).
[53] C. G. Fan, A. Howie, C. A. Walsh, and J. Yuan, Solid State Phenom. B **5**, 15 (1989).
[54] N. Zabala, A. Rivacoba, and P. M. Echenique, Phys. Rev. B **56**, 7623 (1997).
[55] F. J. Garcia de Abajo and J. Aizpurua, Phys. Rev. B **56**, 15 873 (1997).
[56] T. Stockli, J.-M. Bonard, A. Chatelain, Z. L. Wang, and P. Stadelmann, Phys. Rev. B **57**, 15 599 (1998).
[57] J. Thirwell, Proc. Phys. Soc. London **91**, 552 (1967).
[58] N. E. Christensen and B. O. Seraphin, Phys. Rev. B **4**, 3321 (1971).
[59] C. J. Powell, Phys. Rev. B **175**, 972 (1968).
[60] J. C. Ingram, K. W. Nebesny, and J. E. Pemberton, Appl. Surf. Sci. **44**, 293 (1990).
[61] H. Yoshikawa, Y. Irokawa, and R. Shimizu, J. Vac. Sci. Technol. A **13**, 1984 (1995).
[62] T. Nagatomi, R. Shimizu, and R. H. Ritchie, J. Appl. Phys. **85**, 4231 (1999). The correct spectrum for Fig. 1(a) is given by Figs. 4 and 5(a) in the Ph.D. thesis by T. Nagatomi, Osaka University, 1998.
[63] T. Nagatomi, T. Kawano, H. Fujii, E. Kusumoto, and R. Shimizu, Surf. Sci. **416**, 184 (1998).
[64] N. D. Lang, Solid State Phys. **28**, 225 (1973).
[65] T. Nagatomi, R. Shimizu, and R. H. Ritchie, Surf. Sci. **419**, 158 (1999).
[66] W. Plummer, K. D. Tsuei, and B. O. Kim, Nucl. Instrum. Methods Phys. Res. B **96**, 448 (1995).